Tunneling States of OH^- in KCl Crystals

W. E. Bron* and R. W. Dreyfus
IBM Watson Research Center, Yorktown Heights, New York
(Received 5 December 1966; revised manuscript received 1 May 1967)

Energy levels of OH^- in KCl crystals are evaluated from transitions due to resonant absorption of electromagnetic energy. These transitions are interpreted in a consistent way through a model in which the OH^- moves in a 3-dimensional set of harmonic potentials. With respect to the lowest set of energy levels, i.e., those due to tunneling, microwave absorption measurements show that the splitting factor equals 5.5 ± 1.1 kMc/sec and the apparent dipole moment of this system equals 3.3 ± 0.6 Debye units$=0.69\pm0.12$ eÅ. Furthermore, a combination of the present microwave absorption results with infrared spectra shows that the center of mass of the OH^- ion is displaced 0.3 Å from the halide lattice site. Before carrying out the above calculations, the effects of actual experimental conditions upon microwave-power absorption were evaluated. Such evaluation, including theoretical verification, gives the following results: Saturation of the microwave transitions can be readily achieved in a re-entrant cavity. From this effect, the relaxation time is shown to be $>10^{-7}$ sec at 1.4°K and is limited by single-phonon interactions in the 1.4 to 6° range. Phonon interactions produce negligible broadening below 6°K. OH^- concentrations ≥20 ppm lead to line broadening via a simple (electrostatic) dipole-dipole interaction. In samples with ≤1.4 ppm of OH^- ions, the linebreadth is due to the ($\sim10^7$ dyne/cm^2) stress of grown-in dislocations. Having established the above facts, their deleterious effects were minimized before fitting the data with our model.

I. INTRODUCTION

CONSIDERABLE recent interest has been focused on the vibrational or librational type of motion of dipolar impurities, such as OH^-, within alkali-halide lattices.[1] The motion is controlled by the multi-well crystal-field potential which exists in a substitutional lattice site. For infinitely high-potential maxima, each quantum state is degenerate in accordance with the periodicity of the crystal potential and is best represented by a vibrational state in an isolated-potential well. For less than infinite-potential barriers, these states overlap and thereby introduce small energy splittings. This is the solid-state analog of tunneling within the ammonia-gas molecule. For OH^- in KCl, the lowest manifold of tunneling states, i.e., those arising from the overlap within the lowest vibrational state, possesses energy splittings in the microwave-frequency range.

In our original paper[2] we reported the absorption of 9-kMc/sec-microwave energy due to two resonant electric-dipole transitions between these tunneling states, and the identification of the associated quantum states. The results were consistent with a model in which, in the absence of external fields, the lowest-energy state belongs to the A_{1g} representation, the next highest to the T_{1u} representation, and the next to the E_g representation. This sequence of energy levels agrees with the crystal-field potential minima lying along the cube axes and overlap to primarily occur between wavefunctions localized at nearest-neighbor potential wells. Our estimate of the energy splittings was limited to a knowledge that the zero-field splitting was less than 9 kMc/sec.

Since the publication of our original paper, we have obtained more accurate data, and additional information has been reported by other workers in the field. As a result, we now determine quantitative values for the tunneling splitting δ (of the ground set of states of the OH^- ion rotating in a KCl lattice) and for the effective dipole moment μ of this system. These values are obtained from an analysis of the paraelectric-resonance experiment (i.e., the Stark effect) at various microwave frequencies: at 9 kMc/sec by us,[2] at 24 kMc/sec by Estle and Schearer,[3] and at 35 kMc/sec by Feher, Shepherd, and Shore.[4] Our initial objective is to make a comparison between these δ and μ values and those estimated by Feher *et al.* from the measurements of relative line intensities as observed at a single frequency, 35 kMc/sec.

II. EXPERIMENTAL TECHNIQUES

A. Apparatus

Transitions between tunneling states are achieved through excitation of the crystal with the electric component of a microwave field.[2,4] Alkali-halide samples are placed in the position of highest electric field within a re-entrant cavity so as to obtain the maximum rate of excitation. A schematic illustration of the cavity and the position of the sample are shown in Fig. 1. The re-entrant cavity has the following characteristics and features. A dc electric field is applied to the sample in

* Present address: Department of Physics, Indiana University, Bloomington, Indiana.

[1] See, e.g., W. Känzig, J. Phys. Chem. Solids **23**, 479 (1962); W. Känzig, H. R. Hart, Jr., and S. Roberts, Phys. Rev. Letters **13**, 543 (1964); E. M. Gyorgy, M. D. Sturge, D. B. Fraser, and R. C. LeCraw, *ibid.* **15**, 19 (1965); U. Kuhn and F. Lüty, Solid State Commun. **3**, 31 (1965); H. S. Sack and M. C. Moriarty, *ibid.* **3**, 93 (1965); W. D. Seward and V. Narayanamurti, Phys. Rev. **148**, 463 (1966); V. Narayanamurti, W. D. Seward, and R. O. Pohl, *ibid.* **148**, 481 (1966).

[2] W. E. Bron and R. W. Dreyfus, Phys. Rev. Letters **16**, 165 (1966); Addendum, *ibid.* **17**, 689 (1966); Bull. Am. Phys. Soc. **11**, 73 (1966).

[3] T. L. Estle and L. D. Schearer (private communication). This measurement was made on a piece of the 1.4 ppm material described in Table I.

[4] G. Feher, I. W. Shepherd, and H. B. Shore, Phys. Rev. Letters **16**, 500 (1966); Erratum, **16**, 1187 (1966).

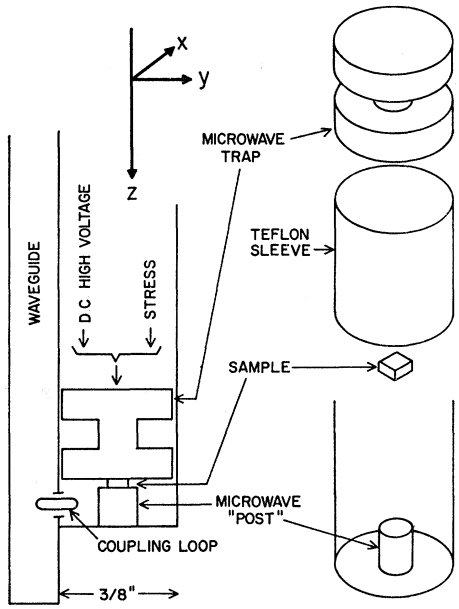

FIG. 1. A schematic illustration of the microwave cavity used to observe paraelectric resonance. Some of the dimensions are as follows: the microwave post is 3.18 mm in diam and 4 mm high; the teflon sleeve is 0.254 mm thick and the samples are about 2 mm² in area with an 0.6 mm thickness producing resonance at 10 kMc/sec, 0.45 mm giving 9 kMc/sec and 0.33 giving 8 kMc/sec.

order to perturb the energy levels to resonance with the microwave energy. This is accomplished by "cutting" the cavity as shown, blocking the microwaves by means of a trap, and inserting a Teflon sleeve around the trap in order to isolate the dc voltage. Since the trap slides against the cavity walls, calibrated springs or an adjustable plunger can be used to apply an axial stress to the sample. Figure 1 shows that both the stress and electric fields point along the z axis. (We take note of this point by hereafter referring to the electric field as E_z.) The fact that the re-entrant cavity operates in its fundamental mode means that the microwave electric field is also parallel to the z axis. With samples $\lesssim$1.4 ppm of OH^- ions, the Q of the cavity is 2000 in the liquid-helium-temperature range.

Phonon-induced broadening of a resonance line is essentially eliminated by performing the experiment with the cavity mounted directly in a liquid-helium Dewar. Pumping on liquid helium produces temperatures between 1.4 and 4°K, as measured by the vapor pressure of the helium. Temperatures greater than 4.2°K are obtained with a resistance heater after the liquid helium level drops below the cavity. The temperature of the cavity is then measured by a copper-constantan thermocouple, the cold junction of which extends ~20 cm below the cavity and into the remaining helium.[5] We estimate the maximum error in this technique to be ±1°K and to occur in the 5–8°K range.

[5] Appropriate calibration tables are given by R. L. Powell, M. D. Bunch and R. J. Corruccine, Cryogenics 1, 139 (1961).

The electronic equipment external to the cavity is the electric-field analog of the conventional electron-paramagnetic-resonance spectrometer. A Varian spectrometer is used which contains an 8–10 kMc/sec klystron, a microwave bridge, an automatic frequency control, a field-modulation amplifier and an associated lock-in amplifier. Instead of an external magnet, a high-voltage dc supply is used. To the output of the latter a 200 cps modulation voltage is added by means of a 1:10 step-up transformer. Modulation fields range from 0.1 to 0.7 kV/cm. The microwave bridge is operated in the "high-power" mode with the klystron frequency locked to the re-entrant cavity. Microwave power is measured at the 20-dB coupling point of the bridge, and then multiplied by 100 to give the input power.

B. Samples

The samples listed in Table I were grown by the Kyropoulus method under an argon atmosphere.[6] Table I lists the starting KCl material and the technique of adding KOH. A platinum crucible held all the melts with the exception of the KCl: (0.3 ppm) KOH sample, for which a fused-silica crucible was used. After growing, the samples were cooled to room temperature in ~16 h, cleaved to size, and utilized without further heat treatment.

Impurities were estimated on the basis of the following techniques. The work of Fritz, Lüty, and Anger[7] was used to determine the KOH concentration from the ultraviolet absorption band at 204 mμ. The divalent metallic-impurity content, virtually entirely calcium ions, was determined from spectrographic analysis and ionic-conductivity measurement.

The strain averaged over the volume of the sample is calculated[8] to be 7×10^6 dyn/cm² for a dislocation count[9] of 2×10^6/cm². For present purposes, it suffices to take the stress as $\sigma_{rr}(\sigma_{\theta\theta})$ from Eq. (19.6) of Ref. 8

$$\sigma_{rr}=\sigma_{\theta\theta}=-Gb\,(\sin\theta)/4\pi(1-\nu)r \qquad (1)$$

The following quantities are substituted into (1): $G=1.68\times10^{11}$ dyn/cm², $b=4.43$ Å, $\nu=0.3$, the average of $\sin\theta\,|_0^\pi=2/\pi$, and the number of dislocations/cm²$=\frac{1}{2}\pi r^2$. From Eq. (19.4) of Ref. 8, one sees that $\sigma_{r\theta}$ for a screw dislocation has this same average value within 10%.

III. EXPERIMENTAL RESULTS AND INTERPRETATION

The primary objective of the present paraelectric-resonance work is the acquisition of experimental data

[6] A description of the apparatus is given in *The Art and Science of Crystal Growth*, edited by J. J. Gillman (John Wiley & Sons, Inc., New York, 1963), p. 410.

[7] B. Fritz, F. Lüty, and J. Anger, Z. Physik **174**, 240 (1963).

[8] C. Kittel, *Introduction to Solid State Physics* (John Wiley & Sons, Inc., New York, 1956), 2nd ed., pp. 540–546.

[9] The dislocation etching technique is given by S. Mendelson, J. Appl. Phys. **32**, 1579 (1961).

TABLE I. Characterization of samples.

Concentration of KOH (ppm)[a]	Starting KCl	Method of adding KOH	Ca^{2+} concentration (ppm)	Dislocation count[b] (No./cm²)
1000	Vacuum dried	KOH pellet	~10	8×10^6
20	Vacuum dried	Dilution of 1000 ppm sample	3	8×10^6
20	Zone refined	Dilution of 1000 ppm sample	<1	2×10^6
1.4	Zone refined	Dilution of 1000 ppm sample	≪1	2×10^6
0.3	Zone refined	Harshaw seed crystal	0.1	8×10^6

[a] As determined from the 204-mμ absorption band.

[b] This count pertains to an unstrained surface (and hence bulk of the crystal) which was exposed by dissolving away part of the crystal with water. Cleaved surfaces have a dislocation count of ~10^8/cm² and the damage extends 0.02 to 0.04 mm into the crystal.

which reflects the behavior of *isolated* OH^- ions in KCl crystals. It should be recognized that OH^- dipoles are unusually sensitive to long-range interactions because of their large electric- and stress-dipole moments. An example of this, given in the next section, is that line broadening and shifting arise when the OH^- concentration is raised to 20 ppm. Furthermore, there existed a difference in the exact line position (in terms of electric field) in the data reported by us as compared to Feher *et al.*,[10] and we wished to resolve this difference. This point should not be overemphasized, however, because agreement exists between the papers on the basic points: The origin of the microwave absorption is due to electric-dipole transitions between tunneling states, and two electric-dipole transitions are observed with 9 kMc/sec microwaves. We therefore turn now to a detailed study of the origin of external effects upon the OH^- paraelectric-resonance spectra.

A. Impurity Concentration Effects

As a first step in this study, we note the effect of impurity content on the resonance spectra.[11] The derivative signal of the microwave power absorbed is found to be proportional to the 204-mμ absorption of OH^- in KCl to within a factor of 2. This is an indication that the resonance signal is indeed due to OH^- ions.

The shape of the microwave absorption line is found, however, to depend on the OH^- concentration. The largest changes in the line shape occur at the highest concentrations of dipolar impurities. This condition is reached at relatively low concentrations for impurities with large dipole moments such as the OH^- ion. Figure 2 shows the line shapes for concentrations in the 0.3- to 20-ppm range. The first band, low E_z, is easily observed and has been identified by us to result from the $2A_1 \rightarrow 3A_1$ transition.[2] (We have adopted here the notation used by Feher *et al.*[4] for the various quantum levels, see also Fig. 7 below.) The second band is not as easily resolved, but through the use of applied strain fields has been identified to result from the $1A_1 \rightarrow 2A_1$ transition. This transition appears to be particularly sensitive to concentration, and is not resolvable when 20 ppm of OH^- ions are present. At this same concentration, the $2A_1 \rightarrow 3A_1$ transition is broadened slightly more than 1 kV/cm.

We propose that the distinct changes seen in the 20-ppm range are attributable to long-range electric fields from other dipoles within the crystal. Such fields are not identical at every point in the crystal and therefore are a source for inhomogeneous broadening of the resonance lines. The following calculation, based on simple classical considerations, supports this idea. A classical calculation is applicable since quantum effects will be small for two dipoles interacting at distances r of ~100 Å. Specifically, overlap of the two hindered-

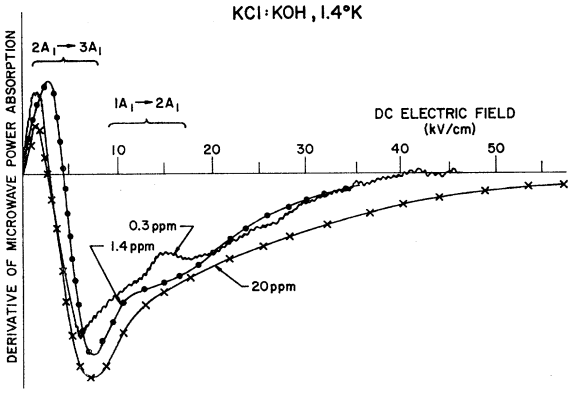

FIG. 2. Relationship between line shape and concentration for KCl: KOH. In particular, note that the $1A_1 \rightarrow 2A_1$ transition is unobservable at 20 ppm of OH^-. The magnitudes of the curves have been magnified by 1, 25, and 200 times for the 20, 1.4, and 0.3 ppm samples, respectively.

[10] The work by Feher *et al.* at 9 kMc/sec is given in the note added in proof to their paper (Ref. 4).

[11] In this section as well as in the following sections we report on measurements at 1.4°K, microwave-power level of $10^{-4}W$ and minimum external stress unless otherwise stated. The microwave trap (Fig. 1) rests on the sample and does exert a stress of 6×10^5 dyn/cm². This stress is negligible compared to the internal stresses due to dislocations, cf. Sec. II B.

rotor wavefunctions is negligible. At these separations, van der Waal's interactions also become negligible, since these fall off as r^{-6}. The interaction is therefore calculated on the basis of one (classical) electric dipole interacting with another. This interaction decreases as r^{-2} and hence represents a long-range interaction.

The starting point for a calculation of the average inhomogeneous field is the well-known formula for the potential v generated by a point dipole

$$v=(\mu/4\pi\kappa\epsilon_0)(\cos\theta/r^2), \tag{2}$$

where μ is the dipole moment, $\kappa\epsilon_0$ is the dielectric constant of the medium, and θ is the angle between the axis of the dipole and the vector $\mathbf{r}$, from the dipole to the point at which v is measured. Since $E=-\text{grad}v$, its average magnitude $\bar{E}$ over a sphere of radius r is

$$\bar{E}=1.6\mu/(4\pi\kappa\epsilon_0 r^3). \tag{3}$$

The value of r(cm) is set equal to $(4\pi C\times 1.6\times 10^{22}/3)^{-1/3}$ the average distance to the nearest impurity, and $\mu=0.69\ e$Å

$$\bar{E}=6.2\times 10^{21}\,\mu C/\kappa\epsilon_0$$
$$=2.5\times 10^4 C \quad \text{kV/cm}, \tag{4}$$

where C is the molar concentration of OH^- ions. For 20 ppm we therefore anticipate a broadening $\bar{E}=\pm 0.5$ kV/cm, + or − since the z component of this field either adds to or subtracts from E_z. This result compares favorably with the observed broadening of 1 kV/cm of the $2A_1\rightarrow 3A_1$ transition in this concentration range.

In addition to the electric fields of OH^- dipoles, two other effects could contribute to the inhomogeneous line broadening. First, pairs of OH^- ions may interact through their mechanical dipole moments. Second, either electric field not pointing exactly along the [001] axis will increase the number of allowed transitions beyond $1A_1\rightarrow 2A_1$ and $2A_1\rightarrow 3A_1$ (and $1A_1\rightarrow 3A_1$ if one considers the range $\mu E>\delta$). Because of the numerical agreement of Eq. (4) with experiment, we shall not undertake these additional calculations at this time.

Besides the direct effect of OH^- concentration, other complexes are generated by the presence of OH^- in these crystals. For instance, 3ppm of $CaCl_2$ were grown into one KCl:KOH crystal (see Table I) in order to form $Ca(OH)_2$ centers.[7] Only one change is observed in the spectra, in that somewhat broader resonance lines are obtained compared to those from samples which contain only 20 ppm of OH^- ions. Within our model this additional broadening can be expected from the presence of the additional dipoles. However, no new lines are discerned in this case; thus it appears that $Ca(OH)_2$ centers do not exhibit paraelectric resonance at 9 kMc/sec.

Since the submission of the present work, a new paraelectric center has been observed (at 35 kMc/sec) in some KCl:KOH crystals.[12] This new center (hereafter referred to as the HBW center) is reported not to be due to OH^- dipoles. In order to ascertain what effect this HBW center may be producing at 9 kMc/sec, we fabricated a sample which was essentially identical to *d*) of Ref. 12. The signal due to OH^- dipoles, such as is shown in Fig. 2, remains essentially constant in magnitude. However, a large negative-derivative signal appears in the region around 5 kV/cm. This new resonance signal is similar to the 18.5-mW results of Fig. 4 and is produced by the HBW center for all power levels. This is in contrast to the behavior of as-grown KCl:KOH samples, where the power level controls the appearance of the spectra. Further discussion of these points remains for the next section.

B. Microwave Power

We turn now to the effect of microwave power on the spectra of as-grown KCl:KOH samples; this is illustrated in Fig. 3. The spectra are noted to shift from the OH^- spectrum at the low power level to a broad negative signal at the 18.5 mW power level. (As mentioned above, this latter curve is similar to the results obtained from the HBW center.) The change with power level is explained on the following basis. At low power levels, the OH^- spectrum is predominate because of the relatively high concentration of this intentionally added impurity. However, as the power level is increased, the OH^- signal remains constant in magnitude since it represents an essentially saturated transition. The HBW center produces the predominate effect at high power levels as the signal from this center apparently approaches saturation only in the much higher 3.5- to 18.5-mW range. The HBW center is apparently present in most KCl crystals, although, as seen above, the present results (at low power levels) have not been seriously influenced by this contaminant.

The purely negative signal associated with the HBW center means that we have not spanned the entire resonance peak but are only on the side of the peak. The side of the peak which we are observing must be the low-energy side, hence the tunneling state associated with the HBW center has a zero-field splitting larger than the energy of 9-kMc/sec photons.

It may be noted that the 0.1-mW curve is similar to Fig. 3 of Ref. 4, whereas the intermediate power curves are similar to the data reported in Ref. 2. It appears, therefore, that the differences between the experimental

[12] (This reference was added in proof.) G. Höcherl, D. Blumenstock, and H. C. Wolf, Phys. Letters **24A**, 511 (1967). This reference strongly suggests that the sharp line reported at 7kV/cm in Ref. 4 is not due to OH^- dipoles. Under the condition that this criticism is valid, the position (in terms of E_z) of the $2A_1\rightarrow 3A_1$ absorption still provides an estimate of the tunneling splitting, δ. Even further, the value of δ as determined in the present work represents a definite upper limit to the range of acceptable δ values.

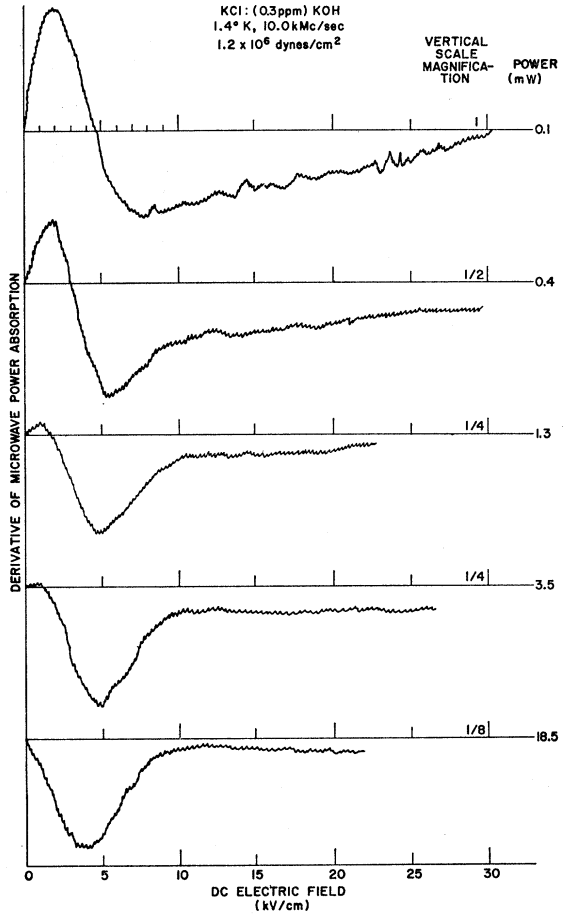

FIG. 3. The observed paraelectric-resonance signal as a function of power dissipated in the microwave cavity. The signal observed at 0.1 mW represents the true absorption mode. With respect to this true absorption mode, it may be noted that the $1A_1 \rightarrow 2A_1$ transition is unobservable because the frequency is $\sim$10 kMc/sec. With low uniaxial stress, such as this case, and at frequencies >9 kMc/sec, the $1A_1 \rightarrow 2A_1$ transition is difficult to resolve. Contrast the present 10 kMc/sec spectra with the enhanced resolution shown by the 8.1 kMc/sec curve of Fig. 4 (at 1.4°K).

results of Feher *et al.*[10] and those reported earlier by us may simply be the result of the use of different power levels by the two groups.

C. Temperature

Figure 4 shows that the linewidths are similar for 1.4, 4, and 6°K. Because we are dealing with $\sim$0.3-cm^{-1} photons (equivalent to $\sim$0.4°K and not of energies $\gg kT$), any phonon absorption or emission must involve the occupation probability of low lying phonon states. All such probability terms involve T^n dependences[13] with $n \geq 1$. However, since the linewidths are independent of temperature for $T \leq 6$°K, we conclude that interactions with lattice phonons, i.e., thermal energy, are not producing the finite linewidths. This is another way of stating that, for $T < 6$°K, inhomogeneous line broadening is present.

The changes in line shape due to increasing temperature above 6°K are also shown in Fig. 4. In the 9 to 12°K range, the absorption attributed to the $2A_1 \rightarrow 3A_1$ transition essentially disappears. Therefore, in this temperature range the relaxation rate τ_R^{-1}, approaches ω, i.e., $\sim 6 \times 10^{10}$ sec^{-1}. The strong temperature dependence of the linewidth in the 9 to 12°K range implies a strong temperature dependence of τ_R. A similar result at 12°K was obtained by Feher *et al.*[4] in the measurements with 35.4-kMc/sec microwaves. It appears that in this temperature range τ_R varies more rapidly with temperature than T^{-1}, so that we deduce that multiphonon processes predominate.[13] This conclusion is in agreement with the theoretical results of Vredevoe.[14]

Below 6°K, the saturated nature of the $2A_1 \rightarrow 3A_1$ transition indicates the lifetime versus temperature dependence. The relationship between maximum power p absorbed by a line and the lifetime of the excited state τ_R is essentially given by Townes and Schawlow[15] as

$$p \approx (h\nu)^2 n_0 / kT\tau_R. \quad (5)$$

Here p can be taken as proportional to the derivative

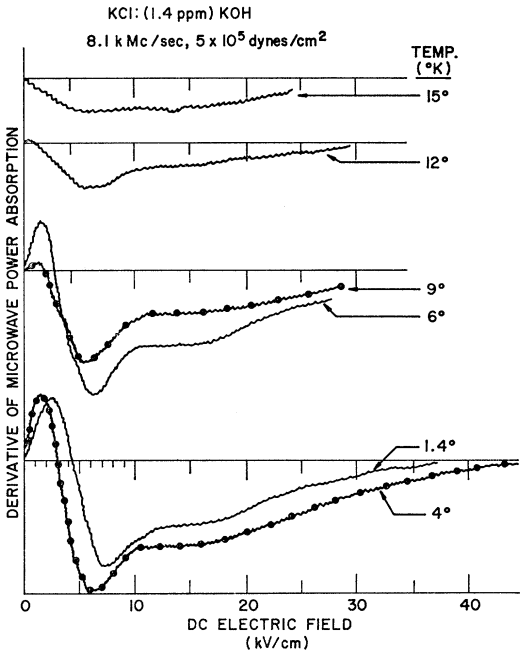

FIG. 4. The resonance signal of KCl:KOH as a function of temperature. Both the $2A_1 \rightarrow 3A_1$ transition near 4 kV/cm and the $1A_1 \rightarrow 2A_1$ transition near 12 kV/cm are significantly broadened at 9° and 12°K. Also note that the $2A_1 \rightarrow 3A_1$ transitions have constant magnitude (within experimental uncertainty) for $T = 1.4$, 4, and 6°K.

[13] J. A. Sussman, Physik Kondensierten Materie **2**, 146 (1964).

[14] L. A. Vredevoe, Phys. Rev. **153**, 312 (1966).

[15] C. Townes and C. Schawlow, *Microwave Spectroscopy* (McGraw-Hill Book Company, Inc., New York, 1955), Eqs. (13–77).

signal since the line shape will not change in the temperature range discussed below. $h\nu$ is the energy of a microwave photon, n_0 is the number of (OH^- ions in the $2A_1$ state) excitable centers in the sample, and kT has the usual significance. As exemplified by the curves at $T=1.4$, 4, and 6°K in Fig. 4, p is independent of T within experimental error. According to the above equation, this independence is obtained only for $\tau_R \propto T^{-1}$. The relaxation of the dipole therefore occurs by interaction with a single phonon.[13,14] Since the $2A_1 \rightarrow 3A_1$ transition is seen to be saturated (cf. Fig. 4) at 0.1 mW, Eq. (5) indicates that $\tau_R > 10^{-7}$ sec. Furthermore, the peak power absorbed by the $2A_1 \rightarrow 3A_1$ transition was derived from an empirical calibration of the resonance equipment. The value so derived was inserted into Eq. (5) and an estimate of $\tau_R = 3 \times 10^{-6\pm1}$ sec was calculated. These (relatively) large values of τ_R indicate that future experiments may find $\tau_R(T)$ by the use of pulsed electric fields.

D. Stress Fields

Our earlier experiments using externally applied stress fields were conducted on samples containing 20 ppm of OH^-. In view of the dependence of the lineshape on concentration, as noted earlier in this section, we have reinvestigated the effect of applied stress on samples containing 0.3 and 1.4 ppm of OH^-. Furthermore, these new measurements were carried out at low power levels. Part of the results are shown in Fig. 5. The observed effect is identical to that reported previously, namely, the absorption band appearing at high electric fields is displaced to yet higher fields by increasing stress. On the other hand, the peak near 4 kV/cm is not altered in position but decreases in magnitude upon increasing stress.

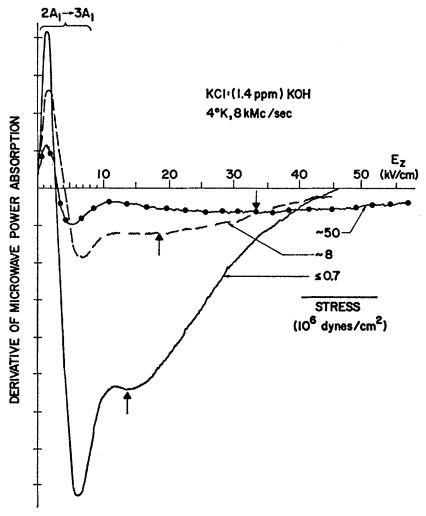

FIG. 5. The effect of [001] stress on the resonance spectra. The position of the maximum negative derivative of the $1A_1 \rightarrow 2A_1$ transition is shown by an arrow. The $2A_1 \rightarrow 3A_1$ transition always appears in the 3 to 4 kV/cm range.

As pointed out in our earlier paper,[2] the above results are consistent only with the assignment of the low-field band to the $2A_1 \rightarrow 3A_1$ transition, and the assignment of the high-field band to the $1A_1 \rightarrow 2A_1$ transition. The actual field position of the peak of the $1A_1 \rightarrow 2A_1$ transition is somewhat in question. This is due to the inability to resolve it from the dominant low-field band, the sensitivity of this band to strain fields, and the fact that with 9-kMc/sec microwaves only a part of the entire absorption band can be observed. This latter point will be discussed in detail in Sec. IV. Nevertheless, the stress dependence of the observable part of the band is the same as that of the entire band.

Next we discuss the question of linewidths in terms of internal stresses. In Sec. IIB the minimum stress due to dislocations in the present samples was shown to be of the order of 7×10^6 dyn/cm². Only the tetragonal (E_g) component of the stress interacts with OH^- centers, whereas the orthorhombic shear component (T_{2g}) and hydrostatic component (A_{1g}) have no first-order effect. In view of this fact, we consider that only one-half of the stress due to dislocations acts upon the OH^- centers. This corrected stress is calibrated in terms of E_z by data such as shown in Fig. 5 for the stress-induced shift of the $1A_1 \rightarrow 2A_1$ transition. The displacements of the lines are then found to be ($\pm$) 2.5 kV/cm. This field is about 50% larger than the linewidths observed in the present experiments. We consider this sufficiently close to verify that dislocations within lightly doped samples are the origin of the inhomogeneous line broadening.

The relationship of linewidth to internal stresses suggests measurements on annealed KCl:KOH crystals. The present work, however, is directed towards finding the dipole moment and energy levels from paraelectric resonance-line positions versus microwave frequency. Since data on annealed samples are not available at the higher frequencies, the above determination is not yet possible.

In summary, the shape and position of the paraelectric resonance line at 9 kMc/sec are available from the present data. The effects of OH^- concentration, internal stresses, and lifetime had been noted and confirmed by simple calculations. These extraneous effects were then minimized by utilizing data taken at 1.4°K, OH^- concentration near 1 ppm, and minimal microwave power. Therefore, the present data correctly represent the paraelectric microwave absorption near 9 kMc/sec for as-grown crystals.

IV. THEORY

First we develop a model for the vibrational and tunneling behavior of OH^- in KCl. This model and associated theory are subsequently extended to include the effect of externally applied electric fields. Application of these theoretical calculations to the experimental data yields values for the tunneling splitting, for the

apparent dipole moment of the system, and for the displacement of the OH^- from the normal lattice site.

A. Tunneling Splitting

The hydroxyl impurity in alkali halides is known to occupy a substitutional halide site in the lattice.[16] As a starting point, we visualize the vibrational motion of the OH^- ion within the lattice site in terms of the following classical model. The OH^- ion is equated to a dipole with positive and negative charges displaced from each other by 0.97 Å. In addition, a positive charge (with radius of 1.33 Å) located at the alkali site of the lattice represents the charge of the cation. A "hard sphere" is taken to represent each ion whose radius is set equal to the usual (Pauling) radius. We then determine that position of the OH^- relative to the alkali ions which gives the lowest electrostatic energy. Within this simple picture, the lowest energy is obtained when the OH^- ion is aligned in a $\langle 100 \rangle$ direction of the lattice, and the oxygen ion and the alkali ion "touch" each other. The center of mass (c.m.) of the OH^- ion is displaced from the lattice site in a $\langle 100 \rangle$ direction by 0.34 Å.

When a radially-dependent repulsive force is substituted for the hard sphere, one finds that a possible vibrational motion involves a translation-rotation (TR) of the OH^- ion within the lattice site.[2] In this motion, the c.m. of the ion undergoes translational motion from one potential well to an equivalent neighboring well. However, the rotation of the molecule is considered to be constrained so that the $O^=$-H^+ bond is always collinear with the line from the c.m. (of the OH^-) to the center of the anion site.

Another type of vibrational motion exists in which the OH^- ion rotates about its c.m. but without translation. The energy levels of this motion must be greater than 19 cm^{-1} (the rotational constant of free OH^-) and hence fall entirely outside of present considerations.

The crystal potential for the TR motion consists of a 3-dimensional series of potential maxima and minima. The measurements of Lüty *et al.*[17] verify the hypothesis that the potential minima must lie along the $\langle 100 \rangle$ directions of the alkali-halide lattice, and presumably[18] the maxima lie along $\langle 111 \rangle$ directions. For OH^- in KCl the potential maxima are known to be very high, and have been estimated by Wedding and Klein[19] to be of the order of 530 cm^{-1}. The classical model, discussed up to this point, actually applies only if the potential maxima are infinite in magnitude. In this event, the ground state of the system, for example, is sixfold degenerate with the OH^- vibrating in one of the six equivalent potential wells.

As is well known, for less than infinite potential maxima the wavefunctions may tunnel through the barrier so that the problem must be treated quantum mechanically. The present quantum-mechanical model is an outgrowth of the work of Gomez, Bowen, and Krumhansl.[20] This model starts with wavefunctions derived from simple harmonic oscillators. The advantages of this model are that the wavefunction overlap, and the OH^- displacement are taken explicitly into account, and a wide range of barrier heights may be treated. Since most of the work of Gomez *et al.*[20] accentuated results pertinent to KCl:LiCl, we have extracted and extended those portions which we require for analysis of the KCl:KOH data.

In the present case, there exist six isotropic harmonic oscillators with the minimum potential displaced an amount χ_i^0 along respective $\langle 100 \rangle$ directions. The position of these minima are indicated by the numbered points in Fig. 6. The potential with respect to the well in the ith direction is simply

$$V_i(\mathbf{r}-\mathbf{r}_i^0)=\tfrac{1}{2}m\Omega^2[(\chi_i-\chi_i^0)^2+\chi_j^2+\chi_k^2], \qquad (6)$$

where χ_i, χ_j, and χ_k are coordinates along $\langle 100 \rangle$ axes, m is the reduced mass of the OH^- ion, and Ω is the harmonic frequency. The displacement will be assumed independent of direction, so that $\chi_i^0=\chi^0$. The utilization of a spherical potential, i.e., isotropic harmonic oscillators, will be justified at the end of this section. In each well the ground-state wave function for a harmonic oscillator can then be written by inspection. The function of the ith well is

$$|i\rangle=f\exp\{-g[(\chi_i-\chi^0)^2+\chi_j^2+\chi_k^2)]\}, \qquad (7)$$

where f is a normalization constant equal to $(m\Omega/\pi\hbar)^{3/4}$ and $g=m\Omega/2\hbar$.

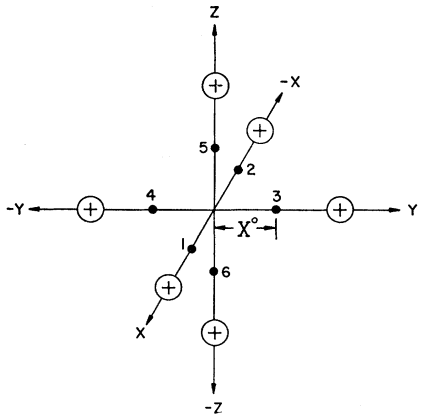

FIG. 6. The positions of the minima of the six isotropic harmonic potentials along the six $\langle 100 \rangle$ directions are indicated by the solid points. The circles with plus signs illustrate the positions of the nearest-neighbor alkali ions.

[16] H. Paus and F. Lüty, Phys. Status Solidi **12**, 341 (1965).
[17] U. Kuhn and F. Lüty, Solid State Commun. **2**, 281 (1964); H. Härtel and F. Lüty, Phys. Status Solidi **12**, 347 (1965).
[18] A. F. Devonshire, Proc. Roy. Soc. (London) **A153**, 601 (1963).
[19] B. Wedding and M. V. Klein, Bull. Am. Phys. Soc. **11**, 228 (1966).
[20] M. Gomez, S. P. Bowen, and J. A. Krumhansl, Phys. Rev. **153**, 1009 (1967); S. P. Bowen, M. Gomez, and J. A. Krumhansl, Phys. Rev. Letters **16**, 1105 (1966).

Each well is next enclosed in a cell, whose boundaries are planes perpendicularly bisecting the lines joining the potential minima of the well to the minima of the neighboring wells. For each well the potential is made zero outside of its boundaries. Depending on the magnitude of Ω and χ_0 above, a certain amount of overlap will occur among the wave functions in Eq. (7). We define

$$S=\langle i\,|\,j\rangle,$$
$$S'=\langle i\,|\,k\rangle, \tag{8}$$

where S and S' are the nearest-neighbor, and next-nearest-neighbor overlap integrals, respectively. A set of normalized and properly symmetrized ground wave functions can then be determined by a method analogous to that used in the Linear Coupling of Atomic Orbital (LOAC) method of ligand-field theory.[21] The appropriate set of functions $\psi_{n\Gamma}$ for the present case is

$$\begin{aligned}
\psi_{1A_{1g}}&=[6(1+4S+S')]^{-1/2}\\
&\quad\times(|\,1\rangle+|\,2\rangle+|\,3\rangle+|\,4\rangle+|\,5\rangle+|\,6\rangle),\\
\psi_{3E_g}&=[12(1-2S+S')]^{-1/2}\\
&\quad\times[|\,1\rangle+|\,2\rangle+|\,3\rangle+|\,4\rangle-2(|\,5\rangle+|\,6\rangle)],\\
\psi_{3E'_g}&=[4(1-2S+S')]^{-1/2}(|\,1\rangle+|\,2\rangle-|\,3\rangle-|\,4\rangle),\\
\psi_{2T_{1u}}&=[4(1-S')]^{-1/2}(|\,1\rangle-|\,2\rangle+|\,3\rangle-|\,4\rangle),\\
\psi_{2T'_{1u}}&=[4(1-S')]^{-1/2}(|\,1\rangle-|\,2\rangle-|\,3\rangle+|\,4\rangle),\\
\psi_{2T''_{1u}}&=[2(1-S')]^{-1/2}(|\,5\rangle-|\,6\rangle).
\end{aligned} \tag{9}$$

The numbers 1 to 6 refer to the wells as indicated in Fig. 6, Γ refers to the representation to which the ψ's are a basis, and n is the index of the associated energy level.

Values for the relative energies of the tunneling states can be readily obtained by determining the matrix elements of the potential-energy part of the Hamiltonian. The values so obtained are

$$\begin{aligned}
W_1&=(E_0+4\alpha+\beta)/(1+4S+S'),\\
W_3&=(E_0-2\alpha+\beta)/(1-2S+S'),\\
W_2&=(E_0-\beta)/(1-S'),
\end{aligned} \tag{10a}$$

where

$$\begin{aligned}
E_0&=\langle i\,|\,V\,|\,i\rangle,\\
\alpha&=\langle i\,|\,V\,|\,j\rangle,\\
\beta&=\langle i\,|\,V\,|\,k\rangle,
\end{aligned} \tag{10b}$$

and V is a sum of the individual potentials V_i, keeping in mind the boundary conditions of these potentials.

For high-potential barriers, i.e., in terms of the present model for high values of Ω and/or χ^0, we anticipate that

$$\beta\ll\alpha,\ S'\ll S\ll 1,\quad\text{and}\quad \alpha>SE_0. \tag{11a}$$

The latter relation is true because $\langle i\,|\,V\,|\,j\rangle$ is greater than $\langle i\,|\,E_0\,|\,j\rangle$ for the present potential-energy configuration. Then the energies (10a) reduce to

$$\begin{aligned}
W_1&\approx E_0-2\delta=E_0+4\alpha,\\
W_3&\approx E_0+\delta=E_0-2\alpha,\\
W_2&\approx E_0,
\end{aligned} \tag{11b}$$

where δ is taken equal to -2α. This reduction of the more general result (10a) is identical to that obtained by several other theoretical treatments.[4,22] Equations (10a) and (11b) show that the tunneling splitting of the ground state is such that the $1A_1$ state lies lowest and is separated from the $3E_g$ and the $2T_{1u}$ states by an amount 3δ and 2δ, respectively, in the limit of very high potential barriers.

B. Effect of External Electric Field

The microwave measurements have been performed in the presence of an externally applied dc electric field. In order to abstract from this data the zero-field tunneling splitting δ we must examine the energy changes in the presence of the electric field. The corresponding matrix elements, for the energy changes of the ground set of states, are simply

$$\langle\psi_{n\Gamma}\,|\,\mathfrak{y}\cdot\mathbf{E}\,|\,\psi_{n'\Gamma'}\rangle, \tag{12}$$

where $n\Gamma$ and $n'\Gamma'$ run over the states (9), $\mathfrak{y}$ is the electric-dipole moment of the system, and $\mathbf{E}$ is the electric field.

We restrict ourselves here to the experimental case of applied fields only in the [001] direction. Furthermore, for analysis of the microwave results we note the fact that for OH^- in KCl the potential barriers are very high, so that the restrictions (11a) apply. We shall justify this point near the end of this section.

Three of the six states associated with functions (9) are uneffected by the field. These are states arising from the $3E'_g$, $2T_{1u}$, and $2T'_{1u}$ states. The remaining three states are coupled by the field, the resulting secular equation being

$$\begin{vmatrix} -2\delta+\Delta & 0 & -\eta \\ 0 & \delta+\Delta & \eta\sqrt{2} \\ -\eta & \eta\sqrt{2} & \Delta \end{vmatrix}=0, \tag{13}$$

where we have made use of Eq. (11b) and have written the differences between the zero-field energies as

$$\begin{aligned}
W_1-W_2&\equiv-2\delta,\\
W_2-W_3&\equiv\delta,
\end{aligned} \tag{14}$$

[21] C. Ballhausen, *Introduction to Ligand Field Theory*, (McGraw-Hill Book Company, Inc., New York, 1962).

[22] H. B. Shore, Phys. Rev. **151**, 570 (1966); M. E. Baur and W. R. Salzman, *ibid.* **151**, 710 (1966); P. Sauer, O. Schirmer, and J. Schneider, Phys. Status Solidi **16**, 79 (1966).

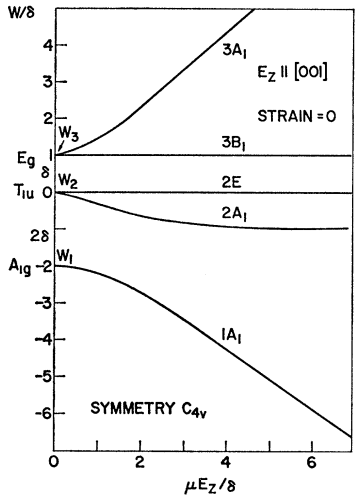

FIG. 7. Energy (W) and group character of the tunneling states as a function of the applied field (E_z). Both the energy of the states and the electric-field energy are given in units of δ.

and we have defined

$$W_2 - W^i \equiv \Delta,$$

where W^i ($i=1, 2, 3$) are the energies in the presence of E_z, and

$$\eta = \tfrac{1}{3}\sqrt{3}\mu E_z.$$

The resultant cubic equation is

$$\Delta^3 - \delta\Delta^2 - (2\delta^2 + 3\eta^2)\Delta + 3\eta^2\delta = 0. \qquad (15)$$

This equation is very simply solved in the limit of infinitely high-potential barriers, i.e., when $\delta \to 0$. Then the solution is

$$\Delta = -\mu E_z, \quad 0, \quad +\mu E_z. \qquad (16)$$

A solution of the more general Eq. (15) has been determined numerically and is plotted in Fig. 7, where the energy of the states and that of the electric field are given in units of δ. The group characters of the various states in the presence of the field are also noted.

In the present case, in which both the dc electric field and the electric component of the microwave field are in the [001] direction of the crystal, electric-dipole transitions are allowed only between states of A_1 character.[23] In the ground set of states, the allowed transitions are accordingly $1A_1 \to 2A_1$, $2A_1 \to 3A_1$, and $1A_1 \to 3A_1$. In Fig. 8 we plot, for fixed values of μ and δ, the energy of these transitions as a function of the dc electric field. Values of μ and δ are so chosen as to give the best fit to the presently available experimental data obtained by us at 9 kMc/sec, those by Estle and Schearer[3] at 24 kMc/sec and those by Feher *et al.*[4] (primarily) at 35 kMc/sec. The result for the transitions $1A_1 \to 2A_1$ (which duplicates $2A_1 \to 3A_1$) and $1A_1 \to 3A_1$ for $\delta = 0$ are shown in dashed lines. Although the number of data points is, at this time, rather limited, the constraints on the two-parameter fit is such that an uncertainty in μ and δ of not more than about 20% is obtained. The values of $\mu = 0.69$ eÅ and $\delta = 5.5 \pm 1.1$ kMc/sec characterize the ground state of OH^- in the present KCl crystals.

The next step is to compare the above values of μ and δ with the results of other measurements. Feher, Shepherd and Shore[4] showed that measurements at a single microwave frequency yield values for δ and μ by means of the following consideration. The transition $1A_{1g} \to 3E_g$ is a (parity-) forbidden electric-dipole transition; however, this restriction breaks down in the presence of an external electric field. In the latter case, the intensity of the transition depends directly on the amount of admixture of opposite parity states and, therefore, depends on δ. From this fact an estimate of δ has been obtained by Feher *et al.* through the measurement of the relative integrated intensity of the $1A_1 \to 3A_1$ transition to that of the presumable composite band due to the $1A_1 \to 2A_1$ and $2A_1 \to 3A_1$ transitions. A comparison of the values obtained by Feher *et al.*[4] to those obtained by us is given in Table II. Besides δ, a value for μ was obtained[4] from the magnitude of the electric field at which the $1A_1 \to 3A_1$ transition appears.

At least two possible sources of internal electric fields might cause inaccuracies in the relative line-intensity technique[4] for determining δ. These sources are local fields due to other impurities and fields set up by the gradients of strain fields around dislocations. However, the agreement shown in Table II reinforces the belief that both methods of determining δ are valid.

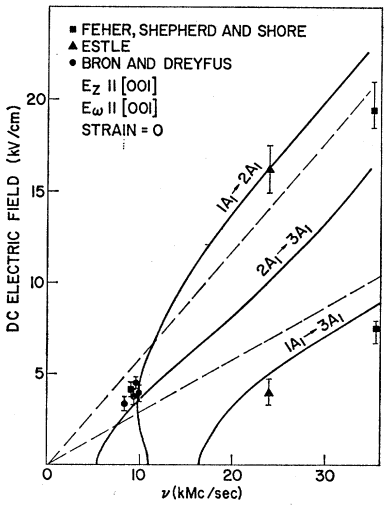

FIG. 8. Frequency (ν) of the allowed transitions as a function of the dc electric field (E_z). E_ω is the microwave-electric field. The asymptotic solutions, i.e., for $\delta = 0$, are shown as dashed lines. The points at 8–10 kMc/sec do not include results for the $1A_1 \to 2A_1$ transition, because this peak is not well resolved (see discussion in the text).

[23] See e.g., J. L. Prather, *Atomic Energy Levels in Crystals*, Natl. Bur. Std. Monograph 19, 59 (1961).

One other point needs to be discussed with regard to the results shown in Fig. 8. To start with, it is clear that with 9-kMc/sec microwaves only the $2A_1 \rightarrow 3A_1$ absorption band can be completely traversed by suitably varying the dc field. Indications of the existence of the transition $1A_1 \rightarrow 2A_1$ can be obtained at this frequency only because the absorption band is quite sensitive to strain broadening. The observed absorption at this microwave frequency is actually limited to that due to the wings of the true absorption band and is accordingly not entered onto Fig. 8. The finite negative-derivative signal due to this $1A_1 \rightarrow 2A_1$ transition may be partly due to the fact that the transition frequency first decreases and then increases as the dc field is increased. This fact has already been pointed out by Feher *et al.*[4] However, the apparent band reflects the electric and strain field dependence of the entire band, a fact which we have used in our earlier paper.

C. OH^- Displacement

We now calculate the displacement of the minima χ^0 of the 3-dimensional harmonic potentials of Eq. (6). It is clear from Eqs. (11a) and (11b) that in the limit of high-potential barriers, the tunneling splitting δ equals -2α, where α is the off-diagonal matrix element of the potential defined in Eq. (10b). This matrix element has been evaluated and is, to terms of first order in magnitude, equal to

$$-\alpha = -\langle i \mid V \mid j \rangle \approx \hbar\Omega\chi^0(m\Omega/\pi\hbar)^{1/2} \times \exp[-3m\Omega\chi^{0^2}/4\hbar]. \quad (17)$$

It is then possible to determine χ^0 from the calculated value of δ above, and a knowledge of the vibrational frequency Ω. This frequency can be obtained from the infrared measurements of Wedding and Klein.[19] They have determined from the side-band structure of the OH^- fundamental stretching vibration that Ω is 5.5×10^{13} rad/sec. Using this value and $\delta = 1.8\times 10^{-17}$ erg (5.5 kMc/sec) we obtain from Eq. (16) a value for χ^0 of 0.28 Å. Anharmonicities in the real crystal potential or a decrease[12] in δ would tend to increase χ^0 slightly, so that it would approach even more closely the value of 0.34 Å obtained from the hard-sphere model mentioned at the beginning of this section. Both numbers lend support to our hypothesis that the OH^- ion is displaced from the normal lattice site.

This displacement helps to explain a part of the difference in the dipole moment of OH^- in KCl as measured in the infrared[7,24] as compared to that measured here and that measured by electrocaloric measurements.[25] The measurement of the infrared absorption attributed to the stretching mode of OH^- in KCl gives an effective dipole moment of only about 0.1 eÅ. In contrast, the effective permanent dipole moment observed in microwave and electrocaloric measurements is in the vicinity of 0.6 to 1.0 eÅ. The latter measurements, however, are influenced by a factor which does not enter into the infrared measurements, namely, the additional dipole moment due to the displacement of the OH^-.

In order to calculate the effects of this charge displacement, the following "centers" (along the O-to-H axis) are given as distances from the oxygen nucleus. The c.m. is at 0.06 Å, the center of positive charge (due to the nine nuclear charges) is at 0.11 Å, and the center of negative charge (due to the ten electrons) is estimated to be located at 0.11 ± 0.02 Å.[26] It is important to note that the additional electron on the $(OH)^-$ ion has further decreased its inherent dipole moment [from the small value the $(OH)^0$ radical had] to essentially zero. This inherent dipole moment is the quantity which controls the infrared absorption and eminently shows that the infrared absorption should be small, just as is observed.[7,23] With respect to the static electric dipole, the extra negative charge gives a moment of 0.25 eÅ. In this way a large fraction of the presently observed dipole moment is accounted for. Part of the remaining difference may lie in the polarization of the lattice by the OH^-.

Now that a quantitative value of χ^0 has been obtained, two of our previous assumptions can be tested. First, consider the nearest-neighbor overlap integral S and the next-nearest-neighbor overlap integral S' as defined in Eq. (8). The values obtained using $\Omega = 5.5\times 10^{13}$ rad/sec and $\chi^0 = 0.3$ Å are $S = 1.6\times 10^{-2}$ and $S' = 9.0\times 10^{-6}$. Since by definition β of Eq. (10b) is smaller than α by a factor of approximately S, we find that the restrictions (11a) are obeyed, so that the approximations of the energies of the ground tunneling states as given in Eq. (11b) are justified for the case of OH^- in KCl.

Second, the effect of a nonspherical potential well is examined with respect to its effect upon the present results. This should be considered since the potential-energy curve involved in motion of the OH^- ion in the radial direction away from (or toward) the K^+ ion is not necessarily identical to the potential-energy curve with respect to the two perpendicular directions of mo-

TABLE II. Comparison of values for zero-field splitting and dipole moment.

	Bron and Dreyfus[a]	Feher *et al.*[b]
Zero-field splitting (kMc/sec)	5.5 ±1.1	6.2 ±0.6
Dipole moment (eÅ)	0.69±0.1	0.88±0.04

[a] Reference 2. [b] Reference 4.

[24] C. K. Chau, M. V. Klein, and B. Wedding, Phys. Rev. Letters 17, 521 (1966).

[25] J. Shepherd and G. Feher, Phys. Rev. Letters 15, 194 (1965).

[26] The center of negative charge in $(OH)^-$ is determined by considering this same quantity in several similar molecules. The requisite data and concepts are given by L. Pauling, *Nature of the Chemical Bond* (Cornell University Press, Ithaca, New York, 1948), 2nd ed., Chap. II. In the case of $(OH)^0$, the center of negative charge is at 0.07 Å. The increase in this quantity due to an additional electron is estimated on the basis of the center of negative charge in molecules such as HF, HN, and BeO.

tion. As noted above, in the limit of high-barrier height, the tunneling splitting equals -2α. If, instead of a spherical potential, an ellipsoidal potential is utilized, we find that α is again given by Eq. (17). Correction terms to this expression do not become important until the ratio of semimajor axis to semiminor axis exceeds 4.5:1. The values of the displacement χ^0 and the tunneling splitting δ calculated on the basis of a spherical potential should accordingly be a very good approximation even to rather nonspherical potentials.

V. CONCLUSION

The paraelectric-resonance results are interpretable in a consistent way through a model in which the OH^- ion moves in a 3-dimensional set of harmonic potentials. The zero-field-energy splitting and the dipole moment, calculated from this model, agree with the values obtained in a number of other experiments. The results further support the concept that the c.m. of the OH^- is displaced from the alkali-halide lattice site.

ACKNOWLEDGMENTS

The authors are indebted to J. D. Axe, R. Rosenberg, T. Schultz, N. Shiren, and R. Title for helpful discussions, and T. L. Estle for making available his experimental results prior to publication. The work of R. W. Dreyfus was partially supported by the U.S. Atomic Energy Commission.

PHYSICAL REVIEW VOLUME 163, NUMBER 2 10 NOVEMBER 1967

Mössbauer Effect in Ir^{193} in Intermetallic Compounds and Salts of Iridium* †

U. Atzmony, E. R. Bauminger, D. Lebenbaum, A. Mustachi, and S. Ofer
Department of Physics, The Hebrew University, Jerusalem, Israel
and
J. H. Wernick
Bell Telephone Laboratories, Murray Hill, New Jersey

(Received 6 June 1967)

Recoilless-absorption measurements of the 73-keV γ rays of Ir^{193} have been carried out using an Os^{193} source in metallic form and absorbers of Ir metal, $Fe_{0.99}Ir_{0.01}$, various rare-earth–iridium (RIr_2) intermetallic compounds, and a few trivalent and tetravalent Ir salts. From the measurements, the assignment of spin $\frac{1}{2}$ to the 73-keV level was confirmed, and the ratio of the magnetic moment of this level to the magnetic moment of the ground level was found to be 3.0 ± 0.1. The small value obtained for the magnetic moment of the first excited state can be explained by the core-excitation model of de Shalit. The results yielded a value of $\delta^2=0.37\pm0.06$ for the $E2/M1$ mixing ratio of the 73-keV transition. The absolute values of the internal magnetic fields acting on the Ir nuclei in iron and in the RIr_2 compounds were deduced. The dependence of these fields on the rare-earth element was found to follow approximately the predictions of the Kasuya-Yosida theory on conduction-electron polarization, though an exact fit between this theory and experiment was not obtained. The electric field gradients acting on the Ir nuclei in the hexagonal Os metal lattice, in some Ir salts, and in the various RIr_2 compounds were deduced. Isomer-shift measurements indicate that the sign of $\Delta\langle r^2\rangle$, the difference in the mean-square charge radii between the first excited state and ground state of Ir^{193}, is positive.

INTRODUCTION

It is generally believed that the ferromagnetic interactions in the pure rare-earth metals and in intermetallic compounds containing a rare-earth metal and a diamagnetic metal are essentially indirect interactions between the localized $4f$ electrons of the rare-earth ions via the conduction electrons. According to this model, the effective magnetic field acting on the nucleus of a diamagnetic ion, which is either an impurity in a rare-earth metal or forms with it an intermetallic compound, is produced by the conduction electrons, which are polarized by their interaction with the $4f$ electrons of the rare-earth ions. The main object of the present measurements was to investigate the dependence of the effective magnetic field acting on the nucleus of the nonmagnetic ion on the properties of the rare-earth ion with which it forms an intermetallic compound. In order to achieve this, measurements of the effective field acting on Ir nuclei in various rare-earth intermetallic RIr_2 compounds were carried out.

The investigated RIr_2 compounds belong to the family of the Laves phase compounds of the RM_2 type, where R is a lanthanide ion and M can be one of several possible other ions. These compounds have a cubic unit cell and the point symmetry of the rare-earth sites in them is also cubic. Bozorth *et al.* have carried out magnetiza-

* Supported in part by the Israel National Academy of Sciences.
† Supported in part by the U.S. Air Force, Office of Scientific Research, OAR, under Grant No. AF-EOAR-64-24, through the European Office of Aerospace Research, U.S. Air Force.